

1 **FISHtoFigure: An easy-to-use tool for rapid, multi-target partitioning and analysis of**
2 **sub-cellular mRNA transcripts in smFISH data**

3 Calum Bentley-Abbot^{1,2†}, Rhiannon Heslop¹, Chiara Pirillo³, Matthew C. Sinton¹, Praveena
4 Chandrasegaran¹, Gail McConnell⁴, Ed Roberts³, Edward Hutchinson² and Annette
5 MacLeod¹

6 ¹Wellcome Centre for Integrative Parasitology (WCIP). University of Glasgow, Glasgow,
7 United Kingdom. School of Biodiversity, One Health, Veterinary Medicine (SBOHVM),
8 College of Medical, Veterinary and Life Sciences, University of Glasgow, Glasgow UK.

9 ²MRC – University of Glasgow Centre for Virus Research. University of Glasgow, Glasgow,
10 United Kingdom.

11 ³Beatson Institute for Cancer Research, Glasgow, United Kingdom.

12 ⁴Department of Physics, University of Strathclyde, Glasgow, United Kingdom.

13

14 [†]Corresponding author: c.bentley-abbot.1@research.gla.ac.uk

15

16 **Abstract:**

17 Single molecule fluorescence *in situ* hybridisation (smFISH) has become a valuable
18 tool to investigate the mRNA expression of single cells. However, it requires a considerable
19 amount of bioinformatic expertise to use currently available open-source analytical software
20 packages to extract and analyse quantitative data about transcript expression. Here, we
21 present FISHtoFigure, a new software tool developed specifically for the analysis of mRNA
22 abundance and co-expression in QuPath-quantified, multi-labelled smFISH data.
23 FISHtoFigure facilitates the automated spatial analysis of transcripts of interest, allowing
24 users to analyse populations of cells positive for specific combinations of mRNA targets
25 without the need for bioinformatics expertise. As a proof of concept and to demonstrate the
26 capabilities of this new research tool, we have validated FISHtoFigure in multiple biological
27 systems. We used FISHtoFigure to identify an upregulation of T-cells in the spleens of mice
28 infected with influenza A virus, before analysing more complex data showing crosstalk
29 between microglia and regulatory B-cells in the brains of mice infected with *Trypanosoma*
30 *brucei brucei*. These analyses demonstrate the ease of analysing cell expression profiles
31 using FISHtoFigure and the value of this new tool in the field of smFISH data analysis.

32 **Keywords:** RNAScope, single molecule fluorescence *in situ* hybridisation (smFISH), spatial
33 transcriptomics.

34 **Introduction**

35 Single molecule fluorescence *in situ* hybridisation (smFISH) technologies such as
36 RNAScope enable the visualisation of single mRNA molecules within single cells. mRNA
37 transcripts are detected by fluorescence microscopy, with each transcript appearing as a
38 single 'transcriptional spot' (1). Quantification of these signals enables the analysis of
39 transcriptional activity at the single cell level within the spatial context of tissues (2).
40 However, the large microscopy datasets produced by smFISH experiments currently require
41 custom code in order to conduct in-depth transcriptomic analyses. QuPath is a purpose-built
42 platform for the analysis of large images such as those acquired during smFISH
43 experiments, and is recommended by ACDBio-Techne, the developer of the RNAScope
44 platform (<https://acdbio.com/qupath-rna-ish-analysis>), for image analysis (3). QuPath has
45 specific in-built tools for cell segmentation and fluorescent spot detection, which can be used
46 to quantify transcriptional spots. Furthermore, the software incorporates a batch processing
47 feature which facilitates automated analysis of data from multiple images (3). Following
48 quantification, QuPath can plot quantified data, such as transcripts per cell, as a histogram
49 (3). However, users wishing to conduct more complex analyses, such as differential
50 expression analysis or co-expression analysis, must develop custom pipelines to parse raw
51 QuPath output data, thus restricting such analysis to users with extensive bioinformatics
52 experience.

53 Here, we present FISHtoFigure, a standalone, open-source software tool for the in-
54 depth analysis of transcript abundance in QuPath-quantified smFISH data by users with all
55 levels of bioinformatic experience. FISHtoFigure can concatenate the batch processed data
56 from QuPath, enabling the analysis of large, multi-image datasets. Notably, FISHtoFigure
57 allows users to conduct transcript abundance analysis for cells with specific, multi-transcript
58 expression profiles. Additionally, FISHtoFigure enables users to conduct differential
59 expression analysis between datasets, facilitating the targeted study of differential
60 expression in specific cell types and populations. Thus, FISHtoFigure provides a means for
61 all users to examine mRNA expression of multiple transcripts without the need for custom
62 analysis pipelines.

63 Here, we demonstrate the use of FISHtoFigure in two biological scenarios. First, we
64 used FISHtoFigure to analyse T-cell and B-cell populations in the spleens of influenza A
65 virus (IAV) infected mice, hereafter referred to as the spleen dataset. Second, we
66 demonstrate the capabilities of FISHtoFigure for the analysis of high-plex smFISH data

67 collected from highly ramified, non-round cell types, using a dataset obtained in a recent
68 experiment by our group investigating microglia in the brains of *Trypanosoma brucei brucei*
69 infected mice, hereafter referred to as the brain dataset (4).

70

71 **Materials and Methods**

72 *Specifications, Usage, and Data Handling*

73 FISHtoFigure is a Python-based analytical software tool, designed to quantify cell
74 expression profiles within smFISH data. Expression profile analysis is conducted in
75 FISHtoFigure using the Pandas library (5). A two-branched strategy is used to isolate cellular
76 and subcellular data into two new datasets (**Figure 1A**). Graphical outputs are generated
77 using a combination of the Matplotlib and Seaborn Python libraries (6,7). In addition to the
78 graphical outputs, data from FISHtoFigure analysis are stored in CSV format for downstream
79 statistical analysis. The statistical tests in this paper were performed with GraphPad PRISM.

80 *Sample Collection*

81 All spleen samples were collected from 9 week old, male C57BL/6 mice. A mouse
82 was infected with the IAV A/Puerto Rico/8/34 (PR8; H1N1) and samples were harvested 6
83 days post infection. Samples from an uninfected male C57BL/6 mouse were harvested to act
84 as naïve controls. All brain samples were collected from 6 – 8-week-old, female C57BL/6
85 mice. Two mice were infected with *T. b. brucei* Antat 1.1E (4). Samples were harvested at 45
86 days post infection. Samples from two uninfected female C57BL/6 mice were harvested to
87 act as naïve controls.

88 All samples were fixed in 4% paraformaldehyde (PFA) at room temperature for 24
89 hours and embedded in paraffin. From paraffin blocks, sections were cut on a microtome
90 (Thermo Scientific) and mounted on glass slides for histology. All animal work was carried
91 out in line with the EU Directive 2010/63/eu and Animal (Scientific Procedures) Act 1986,
92 under project licences P72BA642F (Spleen samples) and PC8C3B25C (Brain samples), and
93 was approved by the University of Glasgow Animal Welfare and Ethics Review Board.

94 *RNASeope data collection*

95 Commercial RNASeope control slides containing mouse NIH 3T3 cells (Advanced
96 Cell Diagnostics, US) were used as a positive control sample for RNASeope for all samples.

97 RNAScope was used to visualise *Cd79a* and *Cd4* transcripts in the spleens of naïve and IAV
98 infected mice, and *Cd79a*, *Cx3cr1*, *Il10* and *Il10ra* transcripts in the brain of naïve and *T. b.*
99 *brucei* infected mice. Fresh probe mixes containing the RNAScope probes were prepared for
100 each experiment (**Table 1**). A single probe per channel (C1-C4) was included in each
101 experiment. RNAScope 4-plex positive controls (for *Polr2a*, *Ppib*, and *Ubc*) and negative
102 controls (for the *Bacillus subtilis* bacterial *Dapb* gene) were also included (probe details are
103 listed at <https://acdbio.com/control-slides-and-control-probes-rnascop>). Slides were imaged
104 by confocal microscopy (Zeiss LSM 880, 63x objective for the spleen samples; Zeiss LSM
105 710, 63x objective for the brain samples) within 72 hours of staining.

106 **Table 1. RNAScope targets and detection specifications**

107

Target	Channel	Detection dye	Dye dilution	Detection Channel
<i>Pol2ra</i>	C1	Opal 520	1:1500	FITC
<i>Ppib</i>	C2	Opal 570	1:1500	Cy3
<i>Ubc</i>	C3	Opal 690	1:1500	Cy5.5
<i>Dapb</i>	C1, C2, C3	Opal 520/570/690	1:1500	FITC, Cy3, Cy5.5
<i>Cd79a</i>	C1	Opal 520	1:1500	FITC
<i>Cd4</i>	C4	Opal 650	1:1500	PE/Cy5
<i>Cx3cr1</i>	C2	Opal 650	1:1500	PE/Cy5
<i>Il10</i>	C3	Opal 570	1:750	Cy3
<i>Il10ra</i>	C4	Opal 540	1:1500	FITC/Cy3

108 *QuPath Image analysis*

109 Once imaged, QuPath 0.3.1 Software was used to quantify the number of transcripts
110 for each target probe (3). Negative control images were generated by probing spleen
111 and brain tissue sections with the RNAScope 3-plex negative control probes.
112 Fluorescence measurements for each detection channel in the negative control
113 images were subtracted from final experimental images to determine fluorescence
114 thresholds. Using in-built QuPath annotation tools, one large region of interest (ROI)
115 was specified on each image such that the whole image was encompassed in a
116 single annotation. The “Cell Detection” function was used to determine the number
117 and position of cells in each ROI based on the DAPI nuclear stain (under the
118 assumption that one nucleus represented one cell), and the ‘Subcellular Detection’
119 function was used to calculate the number of transcripts for each target. QuPath

120 output data were then used as input data for FISHtoFigure. The analysis workflow
121 was scripted to enable batch processing of all images within each dataset.

122

123 **Results**

124 We designed FISHtoFigure to facilitate the conversion of QuPath-quantified image
125 data into transcript abundance analytics. We designed a simple graphical user interface and
126 packaged the FISHtoFigure software as a standalone executable program, enabling analysis
127 to be conducted with no interaction with the raw data or underlying Python code. Below we
128 outline the steps involved in analysing smFISH data using FISHtoFigure, along with
129 examples of analysis outcomes.

130 *Step 1: Data Harvesting and Validation of Quantified smFISH Data*

131 First, cellular boundaries and mRNA transcripts were identified using QuPath.
132 QuPath output data were then processed using FISHtoFigure to produce differential
133 transcript abundance analytics for different cell types or expression profiles (3). An overview
134 of the FISHtoFigure pipeline is given in **Figure 1A** and an example of a typical image for
135 processing is given in **Figure 1Bi**.

136 As experiments usually require numerous individual images, we created a dedicated
137 pre-processing tool to concatenate individual QuPath-quantified image datasets into a single
138 file comprising data from any number of smFISH images, which can then be analysed by the
139 main FISHtoFigure program. Due to the volume of information captured during imaging, the
140 resulting quantified files are large and include metrics not relevant for transcript expression
141 analysis (e.g. morphometric data, such as, cell area, nucleus and cytoplasm morphology,
142 etc.). The desired information, i.e., the number of transcripts per cell and fluorescent
143 intensity data, which comprise only a small portion of the quantified data, were extracted by
144 FISHtoFigure from QuPath-quantified smFISH data files and assigned to the cells from
145 which they originate. Metrics were then calculated for each cell, i.e. the number of transcripts
146 and total fluorescent intensities for each mRNA target. In addition to transcriptome
147 information, cell location information is extracted in the form of the cell centroid (based on
148 nuclear staining identified using the “Cell Detection” function in QuPath). These data are
149 then processed by FISHtoFigure using the “Plot Transcript Distribution” feature, which
150 produces a scatter plot of points representing cell centroids, with points sized by number of
151 mRNA transcripts within the cell and coloured by gene (**Figure 1Bii**). This allows users to
152 visualise quantified data in a format analogous to the original smFISH image (**Figure 1Bi**)

153 and, by overlaying this visualised data with the original smFISH image, directly validate the
154 accuracy of data extraction by FISHtoFigure (**Figure 1Biii**).

155 *Step 2: Differential target abundance analysis from smFISH data using the FISHtoFigure*
156 *package*

157 Following data extraction and assignment of transcript information to cells, differential
158 transcript abundance analysis can be conducted using FISHtoFigure's "Transcript
159 abundance analysis" feature.

160 Using our spleen dataset, we investigated T-cell and B-cell populations in the
161 spleens of mice, either uninfected or 6 days after infection with influenza A virus. These cells
162 are highly abundant in spleen tissue and have a classically "round" cellular morphology.
163 Their morphology enabled easy identification of cell boundaries in QuPath, and thus
164 generated a straightforward dataset for software validation. Spleen sections from naïve and
165 infected mice were stained using DAPI to identify cell nuclei and probed for *Cd4* and *Cd79a*
166 mRNA transcripts, enabling us to identify helper T-cells and B-cells, respectively (8,9). This
167 analysis revealed a statistically significant upregulation of *Cd4* expression during infection
168 ($p<0.01$, Mann-Whitney test; **Figure 2A**), while no statistically significant difference in *Cd79a*
169 expression was observed. In addition to graphical outputs, FISHtoFigure analysis is saved in
170 CSV format for further downstream analysis. Here, statistical analysis was performed on the
171 FISHtoFigure output data using GraphPad PRISM.

172 We expanded the analysis capabilities of FISHtoFigure by adding the "Multi-target
173 transcript abundance" feature, enabling the identification and quantification of cell types with
174 multiplex transcriptomic profiles. This feature can be used to identify cells expressing any
175 combination of mRNA transcripts. Here, we used this feature to validate the cell type
176 quantification of our pipeline. *Cd4* and *Cd79a* are well established markers for helper T-cells
177 and B-cells respectively (8,9). Spleen resident B-cells do not express *Cd4*, and T-cells do
178 not express *Cd79a*. Therefore we used the double-positive *Cd4⁺ Cd79a⁺* cell population as a
179 metric for mis-categorisation of cells by FISHtoFigure. The naïve dataset comprised a total
180 of 1229 cells of which 273 contained transcripts of *Cd4* or *Cd79a* (**Figure 2B**). A total of 18
181 cells were labelled as *Cd4⁺ Cd79a⁺*, representing approximately 1.5% of all cells and 6.6% of
182 transcript-expressing cells (**Figure 2C**). The infected dataset comprised a total of 1487 cells
183 of which 882 contained transcripts (**Figure 2B**). The infected dataset showed a higher
184 presumed mis-categorisation rate, with 171 cells (11.5% of all cells and 19.4% of transcript-
185 expressing cells) labelled as *Cd4⁺ Cd79a⁺* (**Figure 2C**).

186 Upon closer inspection of the quantified data, many of the apparently *Cd4⁺ Cd79a⁺*
187 cells contained a majority of transcripts from one gene, suggesting that mis-categorisation

188 typically resulted from a small number of transcripts from the other gene. This could be
189 plausibly explained if incorrect boundary approximations caused a small proportion of
190 transcripts to be mis-allocated between highly localised cells. For example, a B-cell in close
191 proximity to T-cell might appear to contain a single *Cd4* transcript due to cell boundary
192 approximation (**Figure 2D**). In such cases, it is reasonable to assume the cell identity based
193 on the majority transcript. To address this, we introduced a thresholding feature so that
194 users can define the minimum number of transcripts from each mRNA target required for
195 cells to be included in analysis. By setting this threshold at 2 transcripts from each mRNA,
196 the population of *Cd4*⁺ *Cd79a*⁺ cells was eliminated in the naïve dataset and substantially
197 reduced (67 cells, representing 4.5% of all cells and 7.5% of transcript-expressing cells) in
198 the infected dataset (**Figure 2C**). This was consistent with the model that *Cd4*⁺ *Cd79a*⁺ cells
199 were artefacts, and showed that thresholding allowed this source of error to be controlled.

200 Having demonstrated that FISHtoFigure can quantify cell types based on mRNA
201 expression profiles, we progressed to a more challenging system containing cells with less
202 regular boundaries. To do this we examined sections of mouse brains, which contain highly
203 ramified cell types, using data from a study exploring the interactions between regulatory B-
204 cells (Bregs) and microglia during infection with *T. b. brucei* (4). The brain dataset comprised
205 17 images captured from brain sections of infected mice and 9 captured from uninfected
206 (naïve) controls. Brain sections were stained using DAPI and probed for *Cd79a* (a B-cell
207 marker), *Cx3cr1* (a microglia marker), *Il10* (an anti-inflammatory cytokine hypothesised to be
208 involved in Breg–microglia interactions), and *Il10ra* (the receptor for *Il10*) (9,10). These
209 images were quantified in QuPath and concatenated into two datasets comprising naïve
210 control data and infected data.

211 *Cx3cr1* is a well-established microglia marker (10). B-cells do not express *Cx3cr1*
212 and microglia do not express *Cd79a*. Similarly to the spleen dataset, in order to examine to
213 what extent the thresholding function could improve cell type quantification in data containing
214 ramified cells, presumptively mis-categorised *Cd79a*⁺ *Cx3cr1*⁺ cells were quantified. The
215 naïve dataset contained 1631 cells, 914 of which contained transcripts. 30 cells were
216 labelled *Cd79a*⁺ *Cx3cr1*⁺ double-positive (1.8% of all cells, 3.3% of transcript-expressing
217 cells). The infected dataset contained 3907 cells, of which 3332 contained transcripts, 392
218 were labelled as *Cd79a*⁺ *Cx3cr1*⁺ double-positive (10% of all cells, 11.7% of transcript-
219 expressing cells; **Figure 3A**). Applying a threshold of 2 transcripts per mRNA per cell
220 reduced the number of *Cd79a*⁺ *Cx3cr1*⁺ double-positive cells to 4 in the naïve dataset (0.2%
221 of all cells, 0.4% of transcript-expressing cells), and 76 in the infected dataset (1.9% of all
222 cells, 2.3% of transcript-expressing cells; **Figure 3A**). This demonstrated that applying

223 thresholds for transcript abundance could allow accurate allocation of transcripts to cells
224 even for cells with complex and irregular boundaries.

225 Finally, as a demonstration of the application of FISHtoFigure in an experimental
226 workflow, we re-analysed data that we had collected as part of a study of Breg-microglia
227 crosstalk in the brains of mice infected with *T. b. brucei* (4). Briefly, single cell and spatial
228 transcriptomic analyses of infected mice revealed an upregulation of the anti-inflammatory
229 cytokine *Il10*, along with Breg and microglia associated transcripts, in the brains of *T. b.*
230 *brucei* infected mice. We tested the hypothesis that during infection *Il10* expression
231 governed crosstalk between Bregs and microglia in the brain, using smFISH and
232 FISHtoFigure to investigate the localisation of transcripts. FISHtoFigure's "Transcript
233 abundance analysis" function revealed a statistically significant upregulation in *Cd79a* and
234 *Il10* expression in infected specimens compared to naïve controls, in agreement with results
235 from single cell transcriptomics (4). Graphical outputs in the format produced by
236 FISHtoFigure are presented in **Figure 3B** ($p<0.01$, Mann-Whitney test; data from ref (4)).
237 We then used a variety of analyses to validate that this crosstalk was driven by two specific
238 cell types (*Il10⁺* Bregs and *Il10ra⁺* microglia), including visualising these cell types using
239 smFISH. Here, we expand on this analysis by using FISHtoFigure to directly quantify the
240 abundance of two different double-positive cell types in infected and naïve mice. We used
241 FISHtoFigure's "Multi-target transcript abundance" feature to analyse *Cd79a⁺ Il10⁺* Breg
242 populations and *Cx3cr1⁺ Il10ra⁺* microglia populations in naïve and infected specimens. This
243 analysis confirmed that during infection there was an upregulation of both *Cd79a⁺ Il10⁺*
244 Bregs (**Figure 3C**; $p<0.02$, Mann-Whitney test) and *Cx3cr1⁺ Il10ra⁺* microglia (**Figure 3C**;
245 $p<0.01$, Mann-Whitney test). In the context of the current paper, this demonstrates that
246 FISHtoFigure can accurately quantify the abundance of specific cell types, including those
247 with irregular boundaries, using multiplex expression profiles. Taken together, these findings
248 demonstrate the value of FISHtoFigure in an experimental workflow.

249

250 **Discussion**

251 FISHtoFigure automates the extraction and processing of transcriptomic data from
252 QuPath-quantified smFISH data, allowing users to analyse specific transcript expression
253 profiles in datasets that would otherwise be very difficult to parse.

254 Our tool is capable of analysing smFISH data by any number of mRNA targets and
255 quantifying cell types and expression profiles with a high accuracy. Furthermore, the
256 graphical user interface allows users to specify a positivity threshold for transcript
257 abundance analysis (i.e., the number of transcripts required for a cell to be marked as

258 positive, and by extension, be included in analysis), allowing users to directly control the
259 sensitivity of the FISHtoFigure platform individually for each set of analyses.

260 Current analysis packages for smFISH data are largely focused on quantification and
261 labelling of transcripts and only offer limited downstream transcript abundance analysis
262 options, which require bioinformatics experience to implement. For example, *FISH-quant*
263 provides a means to detect transcripts in smFISH data and assign individual transcripts to
264 cells and subcellular compartments (11). *FISH-quant* offers downstream analysis options for
265 mRNA expression, but this analysis is largely focused on the intracellular distributions of
266 transcripts rather than the quantification of cells that express multiple mRNA targets. Another
267 smFISH analysis tool, *dotdotdot*, outputs quantified cell and transcript data in a format
268 interpretable using R or Python. However, bioinformatics experience is required to
269 implement downstream analysis (12).

270 FISHtoFigure facilitates custom differential transcript and cell type abundance
271 analyses without the need for custom code. By providing multi-transcript analysis tools in an
272 intuitive package, FISHtoFigure significantly broadens the accessibility of smFISH analysis.

273 Comparison of FISHtoFigure's spatial distribution plots with the confocal microscopy
274 images from which they were derived demonstrates high levels of concordance between raw
275 and quantified data (**Figure 1B**). We demonstrate that FISHtoFigure can accurately
276 determine cell profiles in different biological systems, and that the in-built thresholding
277 feature can substantially reduce mis-categorisation caused by the close proximity of different
278 cell types (**Figure 2**). In the spleen dataset, applying a threshold of 2 transcripts per mRNA
279 target per cell completely removed all mis-categorised cells in the naïve dataset and reduced
280 mis-categorisation by >60% in the infected dataset (**Figure 2C**). In the brain dataset,
281 applying a threshold of 2 transcripts per mRNA target per cell reduced mis-categorisation of
282 cell types by >80% in both the naïve and infected datasets (**Figure 3A**).

283 In the brain dataset, FISHtoFigure enabled rapid analysis of smFISH data which
284 would otherwise require considerable time investment and bioinformatic experience.
285 FISHtoFigure analysis reveals a statistically significant ($p < 0.01$, Mann-Whitney test)
286 upregulation in expression of *Cd79a* and *Il10* during infection (**Figure 3B**). The ability to
287 analyse and plot cellular information for specific cell types with multiplex transcriptional
288 profiles allowed us to identify the upregulation of *Cd79a*⁺ *Il10*⁺ Bregs and *Cx3cr1*⁺ *Il10ra*⁺
289 microglia in infected specimens compared with controls, a difference which would otherwise
290 require custom code to assess (**Figure 3C**).

291 *Considerations and Limitations*

292 Regarding identifying cell boundaries, QuPath has the capacity to quantify cell
293 boundaries based on a range of factors. Here, cell nuclei were identified via fluorescent
294 DAPI staining, and cell boundaries were approximated by applying a set radius to each
295 identified nucleus using the “Cell Detection” function in QuPath. Though we demonstrate that
296 this can allow the accurate quantification of cells, even for cell types with irregular
297 boundaries, further improvements in the determination of cell boundaries, and by extension
298 cell expression profiles, could likely be achieved through adjustments in sample preparation.
299 For example, for challenging cell types users may wish to experiment with the use of
300 membrane markers to further improve cell boundary quantification.

301

302 **Conclusion**

303 The problem of balancing accessibility for non-specialist users and analytical scope
304 is an important consideration in the development of software tools. Here, we present
305 FISHtoFigure, an analytical platform for QuPath-quantified smFISH data capable of
306 analysing specific cell types and multiplex transcriptomic profiles and of generating a variety
307 of differential transcript abundance analytics for cells expressing a user-specified
308 combination of mRNA transcripts. In the interest of accessibility for users with all levels of
309 bioinformatic experience, we have created a simple graphical user interface and packaged
310 FISHtoFigure as an executable program, thus allowing transcript expression analysis without
311 interaction with raw quantified image data or custom analysis scripts. FISHtoFigure can
312 therefore expand the in-house analysis capabilities of many research groups investigating
313 transcriptomics via smFISH.

314

315 **Acknowledgements**

316 We thank Colin Loney for his assistance in the acquisition of the images forming the
317 spleen dataset used during validation. We also thank Ruaridh Wilson for providing feedback
318 from the perspective of a computational scientist during the writing of this manuscript.

319

320 **Competing Interests**

321 No competing interests were disclosed

322

323 **Grant Information**

324 CBA is funded by a Wellcome Trust Four-Year PhD Studentship in Basic Science
325 [226861/Z/23/Z]. RH is funded by a Wellcome Trust Four-Year Studentship in Basic Science
326 [227095/Z/23/Z]. CP and ER are funded by Cancer Research UK [A_BICR_1920_Roberts]
327 awarded to ER. AML is funded by a Wellcome Trust Senior Research fellowship
328 [209511/Z/17/Z]. PC and MCS are funded by a Wellcome Trust Senior Research fellowship
329 [209511/Z/17/Z] awarded to AML. GM is supported by the UK Medical Research Council
330 [MR/K015583/1], Biotechnology & Biological Sciences Research Council [BB/P02565X/1,
331 BBT011602], and the Leverhulme Trust. E.H. is funded by a Transition Support Award from
332 the UK Medical Research Council [MR/V035789/1].

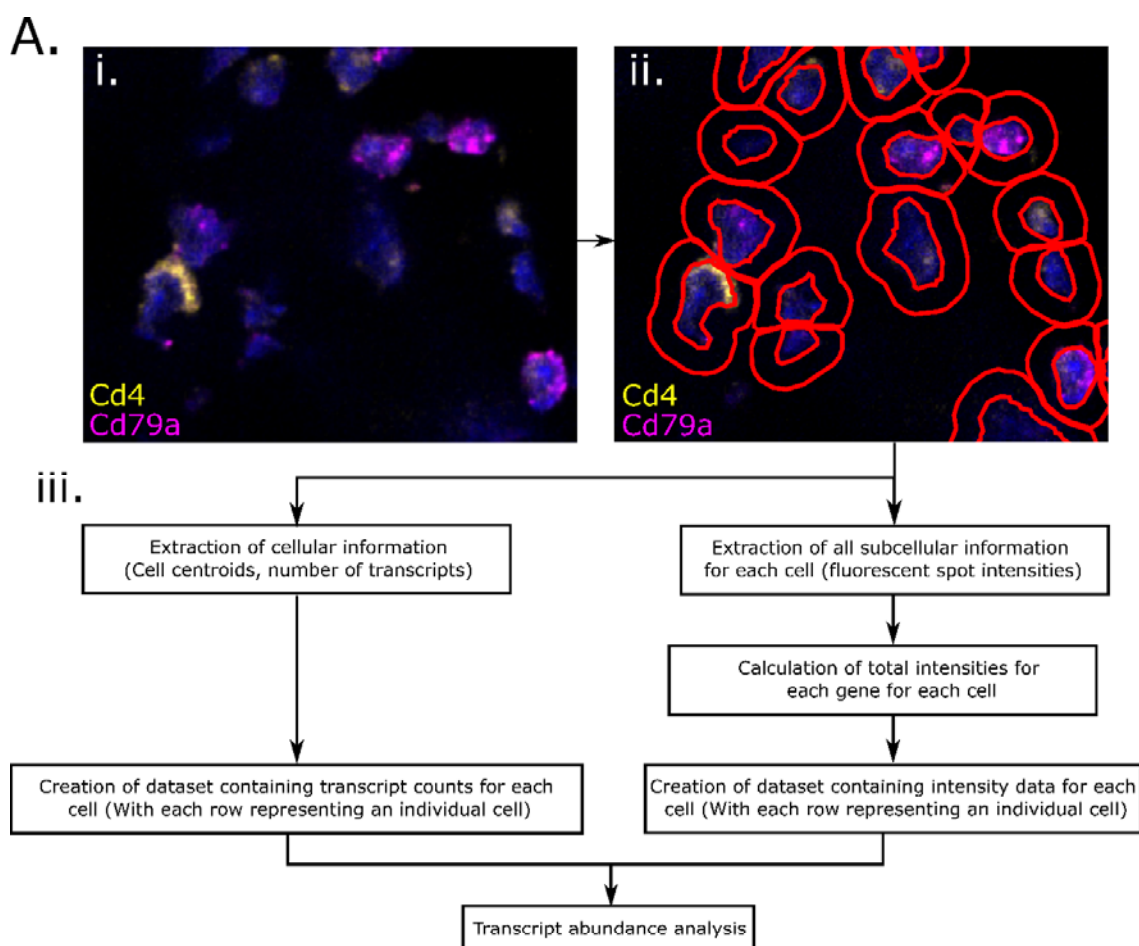
333

334 **Data Availability**

335 All code involved in the production of the FISHtoFigure package and all analysis presented
336 here is available on GitHub: <https://github.com/Calum-Bentley-Abbot/FISHtoFigure.git>
337 Data are available under the terms of the MIT open access licence
338 (<https://opensource.org/license/mit/>).

339

340 **Figure 1**



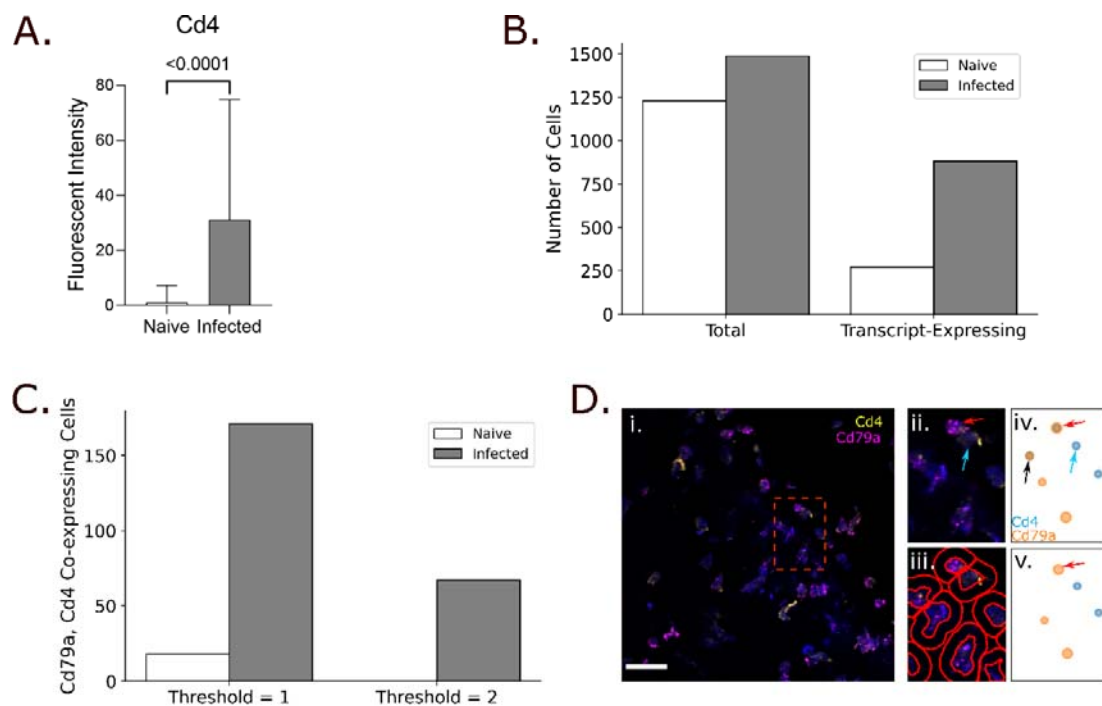
341

342 **Figure 1: FISHtoFigure pipeline. A:** [i] An smFISH image from the spleen dataset captured
343 via confocal microscopy (Zeiss LSM 880). [ii] QuPath's "Cell Detection" function was used to
344 identify cell boundaries (shown in red). Cell nuclei identification is based on fluorescence
345 above background in the channel associated with the nuclear stain (DAPI). [iii] An overview
346 of FISHtoFigure processing of QuPath output data to generate transcript abundance outputs.
347 **B:** [i] An smFISH image from the brain dataset (scale bar = 20 μ m), captured by confocal
348 microscopy (Zeiss LSM 710) and [ii] processed using FISHtoFigure's "Plot transcript

349 distribution" function, where points represent cells and are sized based on the number of
350 transcripts being expressed by that cell. [iii] An overlay of the captured smFISH image with
351 the plot produced by FISHtoFigure demonstrates the accuracy of the pipeline.

352

353 **Figure 2**

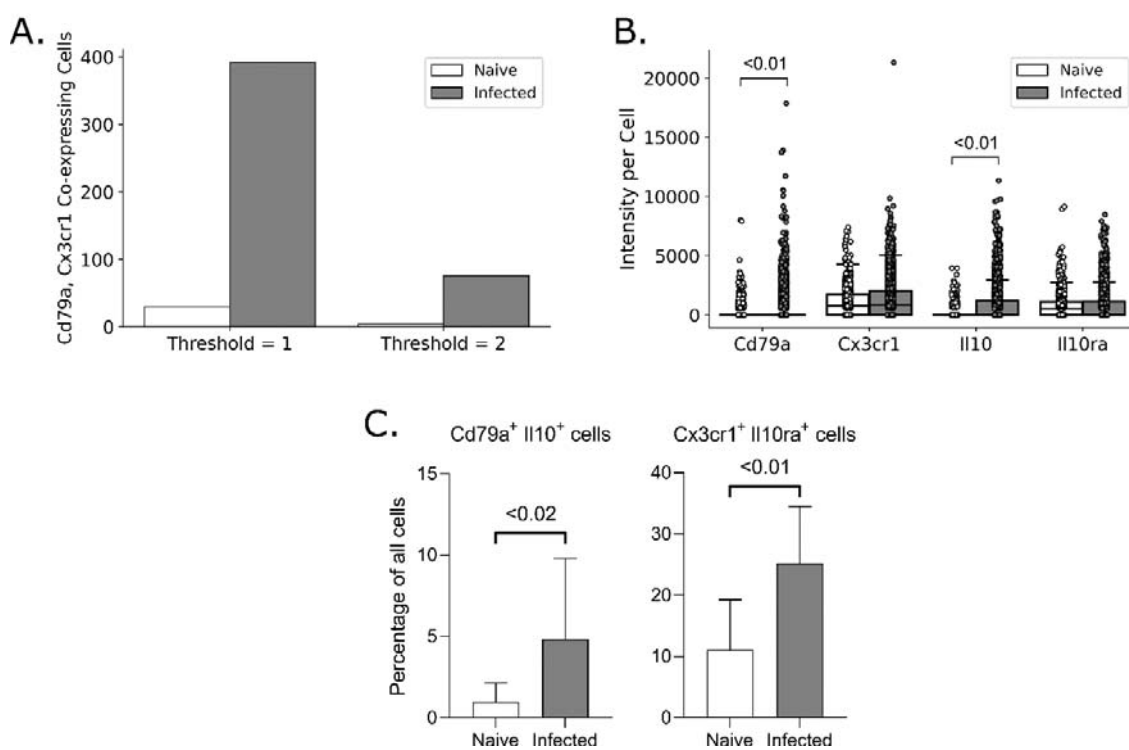


354

355 **Figure 2:** Analysis of spleen samples from naïve and influenza A virus infected mice. **A:**
356 FISHtoFigure quantification of *Cd4* expression in the naïve and infected spleen datasets,
357 significantly upregulated during infection (Mann-Whitney test). **B:** Total number of cells and
358 the number of cells expressing at least one transcript within the naïve and infected spleen
359 datasets. **C:** Number of cells co-expressing *Cd79a* and *Cd4*, with threshold set to 1 or 2
360 transcripts. **D:** [i] An smFISH image from a naïve spleen (scale bar = 20 μ m), captured by
361 confocal microscopy (Zeiss LSM 880). [ii] A zoomed view of the region shown in the red
362 square in [i] shows a B-cell (red arrow) and T-cell (blue arrow) in close proximity. [iii] Cell
363 boundaries identified using QuPath. [iv] FISHtoFigure's "Plot Transcript Distribution" feature
364 with a threshold of 1 transcript per cell, [v] with a threshold of 2 transcripts per cell. Setting a
365 threshold of 2 transcripts per target per cell results in the B-cell being correctly categorised
366 (red arrow) – note the removal of the ambiguous *Cd79a*⁺ *Cd4*⁺ cell expressing both
367 transcripts as they are below threshold levels (black arrow in [iv]).

368

369 **Figure 3**



370

371 **Figure 3:** Examples of FISHtoFigure outputs from analysis of the brain dataset. **A:** Total
372 number of cells expressing both *Cd79a* and *Cx3cr1* with threshold of either 1 or 2 transcripts
373 per mRNA per cell. **B:** Intensities for all cells which express at least one transcript, where
374 each point represents a cell, showing that *Cd79a* and *IL10* expression are significantly
375 upregulated during infection (Mann-Whitney test). Box limits are defined by the interquartile
376 range (IQR) with whiskers extending to the lowest/highest data point still within 1.5 IQR of
377 the lower/upper quartile. This figure re-plots data originally collected in ref (4). **C:** Percentage
378 of cells expressing both *Cd79a* and *IL10* (Bregs) and percentage expressing both *Cx3cr1* and
379 *IL10ra* (Microglia), showing that both are significantly upregulated during infection (Mann-
380 Whitney test). Percentages were taken from each image in the naïve and infected datasets
381 individually and statistical analysis was performed in GraphPad PRISM.

382

383 **References**

1. Wang F, Flanagan J, Su N, Wang LC, Bui S, Nielson A, et al. RNAscope: a novel in situ RNA analysis platform for formalin-fixed, paraffin-embedded tissues. *J Mol Diagn JMD*. 2012 Jan;14(1):22–9.
2. Marx V. Method of the Year: spatially resolved transcriptomics. *Nat Methods*. 2021 Jan;18(1):9–14.

389 3. Bankhead P, Loughrey MB, Fernández JA, Dombrowski Y, McArt DG, Dunne PD, et al.
390 QuPath: Open source software for digital pathology image analysis. *Sci Rep.* 2017 Dec
391 4;7:16878.

392 4. Quintana JF, Chandrasegaran P, Sinton MC, Briggs EM, Otto TD, Heslop R, et al.
393 Single cell and spatial transcriptomic analyses reveal microglia-plasma cell crosstalk in
394 the brain during *Trypanosoma brucei* infection. *Nat Commun.* 2022 Sep 30;13(1):5752.

395 5. Reback J, Jbrockmendel, McKinney W, Van Den Bossche J, Roeschke M, Augspurger
396 T, et al. *pandas-dev/pandas: Pandas 1.4.3* [Internet]. Zenodo; 2022 [cited 2022 Jul 8].
397 Available from: <https://zenodo.org/record/3509134>

398 6. Caswell TA, Droettboom M, Lee A, De Andrade ES, Hoffmann T, Hunter J, et al.
399 *matplotlib/matplotlib: REL: v3.4.3* [Internet]. Zenodo; 2021 [cited 2022 Jul 8]. Available
400 from: <https://zenodo.org/record/5194481>

401 7. Waskom M. *seaborn: statistical data visualization*. *J Open Source Softw.* 2021 Apr
402 6;6(60):3021.

403 8. Luckheeram RV, Zhou R, Verma AD, Xia B. *CD4+T Cells: Differentiation and Functions*.
404 *Clin Dev Immunol.* 2012;2012:925135.

405 9. Mason DY, Cordell JL, Brown MH, Borst J, Jones M, Pulford K, et al. *CD79a: a novel*
406 *marker for B-cell neoplasms in routinely processed tissue samples*. *Blood.* 1995 Aug
407 15;86(4):1453–9.

408 10. Wolf Y, Yona S, Kim KW, Jung S. *Microglia, seen from the CX3CR1 angle*. *Front Cell*
409 *Neurosci.* 2013 Mar 18;7:26.

410 11. Imbert A, Ouyang W, Safieddine A, Coleno E, Zimmer C, Bertrand E, et al. *FISH-quant*
411 *v2: a scalable and modular analysis tool for smFISH image analysis* [Internet]. bioRxiv;
412 2021 [cited 2022 Apr 26]. p. 2021.07.20.453024. Available from:
413 <https://www.biorxiv.org/content/10.1101/2021.07.20.453024v1>

414 12. Maynard KR, Tippani M, Takahashi Y, Phan BN, Hyde TM, Jaffe AE, et al. *dotdotdot: an*
415 *automated approach to quantify multiplex single molecule fluorescent in situ*
416 *hybridization (smFISH) images in complex tissues*. *Nucleic Acids Res.* 2020 Jun
417 19;48(11):e66.

418

419